Published OnlineFirst October 21, 2013; DOI: 10.1158/2326-6066.CIR-13-0067

Cancer Immunology Research

# Locally Delivered CD40 Agonist Antibody Accumulates in Secondary Lymphoid Organs and Eradicates Experimental Disseminated Bladder Cancer

Linda C. Sandin, Anna Orlova, Erika Gustafsson, et al.

*Cancer Immunol Res* 2014;2:80-90. Published OnlineFirst October 21, 2013.

Published OnlineFirst October 21, 2013; DOI: 10.1158/2326-6066.CIR-13-0067

Research Article

Cancer Immunology Research

# Locally Delivered CD40 Agonist Antibody Accumulates in Secondary Lymphoid Organs and Eradicates Experimental Disseminated Bladder Cancer

Linda C. Sandin[1], Anna Orlova[3], Erika Gustafsson[1], Peter Ellmark[4,5], Vladimir Tolmachev[2], Thomas H. Tötterman[1], and Sara M. Mangsbo[1]

## Abstract

Immunotherapy with intratumoral injection of adenoviral vectors expressing CD40L has yielded positive results in experimental and clinical bladder cancer. We therefore hypothesized that anti-CD40 antibody would be effective in this setting. Agonistic CD40 antibodies were developed as vaccine adjuvants but have later been used as treatment of advanced solid tumors and hematologic cancers. Systemic anti-CD40 therapy has been associated with immune-related adverse events, such as cytokine release syndrome and liver toxicity, and local delivery is an attractive approach that could reduce toxicity. Herein, we compared local and systemic anti-CD40 antibody delivery to evaluate efficacy, toxicity, and biodistribution in the experimental MB49 bladder cancer model. Antitumor effects were confirmed in the B16 model. In terms of antitumor efficacy, local anti-CD40 antibody stimulation was superior to systemic therapy at an equivalent dose and CD8 T cells were crucial for tumor growth inhibition. Both administration routes were dependent on host CD40 expression for therapeutic efficacy. *In vivo* biodistribution studies revealed CD40-specific antibody accumulation in the tumor-draining lymph nodes and the spleen, most likely reflecting organs with frequent target antigen-expressing immune cells. Systemic administration led to higher antibody concentrations in the liver and blood compared with local delivery, and was associated with elevated levels of serum haptoglobin. Despite the lack of a slow-release system, local anti-CD40 therapy was dependent on tumor antigen at the injection site for clearance of distant tumors. To summarize, local low-dose administration of anti-CD40 antibody mediates antitumor effects in murine models with reduced toxicity and may represent an attractive treatment alternative in the clinic. *Cancer Immunol Res; 2(1); 80–90. ©2013 AACR.*

## Introduction

In 2008, approximately 380,000 patients worldwide were diagnosed with bladder cancer and 150,000 succumbed to the disease (1). The majority of these patients present with superficial transitional cell carcinoma (Tis, Ta, or T1) that is treated with transurethral resection followed by intravesical chemotherapy, or for high-risk tumors local Bacillus Calmette-Guérin (BCG) immunotherapy (2, 3). BCG treatment induces remission in a majority of patients but is associated with adverse events and 30% to 50% of the patients ultimately fail to respond (4). Radical cystectomy for patients with muscle-invasive bladder cancer results in initial tumor control, but provides a 5-year survival rate of only 40% to 60% due to the presence of micrometastatic disease (2). We have previously shown that local adenoviral CD40L (AdCD40L) as well as CpG therapy can induce systemic antitumor responses in experimental bladder cancer (5, 6). AdCD40L therapy has proven efficient and safe in both humans (7) and dogs (8). Consequently, we wanted to investigate whether local low-dose agonistic CD40 antibody injection could clear experimental bladder cancer. CD40 is expressed by various cell types in the myeloid cell lineage, i.e., dendritic cells, macrophages and monocytes, B cells as well as endothelial cells (9), and dendritic cells are recognized as important targets for anti-CD40 antibody in cancer immunotherapy. Activated dendritic cells can efficiently engulf, process, and present tumor antigen to T cells, resulting in powerful antitumor responses (10, 11). In addition to the antigen-presenting cell (APC)–activating properties of anti-CD40 antibody, CD40 ligation on CD40-expressing tumor cells initiates programmed cell death (12), antibody-dependent cellular cytotoxicity (13), antibody-dependent cellular phagocytosis (14), or complement-mediated cytotoxicity (15), depending on the immunoglobulin G (IgG) subclass.

**Authors' Affiliations:** [1]Department of Immunology, Genetics and Pathology, Division of Clinical Immunology, [2]Department of Radiology, Oncology and Radiation Sciences, Division of Biomedical Radiation Sciences; [3]Department of Medical Chemistry, Preclinical PET Platform, Uppsala University, Uppsala; [4]Alligator Bioscience AB; and [5]Department of Immunotechnology, Lund University, Lund, Sweden

**Note:** Supplementary data for this article are available at Cancer Immunology Research Online (http://cancerimmunolres.aacrjournals.org/).

**Corresponding Author:** Sara Mangsbo, Department of Immunology, Genetics and Pathology, Uppsala University, Rudbeck Laboratory C11, Dag Hammarskjölds väg 20, SE-751 85 Uppsala, Sweden. Phone: +46(0) 18-6119181; Fax: +46(0)18-6110222; E-mail: sara.mangsbo@igp.uu.se

**doi:** 10.1158/2326-6066.CIR-13-0067

Published OnlineFirst October 21, 2013; DOI: 10.1158/2326-6066.CIR-13-0067



Several CD40 agonistic antibodies have been developed for clinical use by the intravenous administration route (16–18). The resulting systemic immune activation has been associated with considerable toxicity, including grade 1 to 2 cytokine release syndrome and transient lymphopenia (16, 19). This study extends the observations of Fransen and colleagues, who compared local low-dose anti-CD40 therapy in combination with the slow-release adjuvant Montanide of virally transformed murine tumors. Local low-dose administration was as effective as systemic high-dose therapy, but with reduced liver toxicity (20). In the current study, we use an experimental bladder cancer model, a tumor well suited for local immunotherapy for which novel therapies are needed to target disseminated disease. We wanted to investigate whether locally administered anti-CD40 antibody could be as efficient as an equivalent dose delivered systemically, and to establish whether the alternative administration route could reduce toxicity. Subsequently, we aimed to pinpoint the effector mechanisms behind the successful local CD40-stimulating immunotherapy for bladder cancer and, lastly, to compare the *in vivo* biodistribution between the two administration routes.

## Materials and Methods

### Cell lines and reagents

The murine bladder transitional cell carcinoma cancer cell line mouse bladder-49 (MB49; a kind gift from Dr. K. Esuvaranathan, National University of Singapore, Singapore in 1996) was cultured in DMEM+ GlutaMax supplemented with 10% FBS, 0.1 mmol/L sodium pyruvate, 100 U/mL penicillin–streptomycin (PEST) at 37°C and 5% $CO_2$. Lewis lung cell carcinoma-1 (LLC-1;American Type Culture Collection) was kept in the same culture medium as MB49. The D1 cell line (21) is a growth factor–dependent immature splenic mouse dendritic cell line cultured in Iscove's modified Dulbecco's medium (IMDM) supplemented with 10% FBS, 100 U/mL PEST, 100 μmol/L β-mercaptoethanol (Invitrogen), and 20 ng/mL recombinant murine granulocyte macrophage colony–stimulating factor (GM-CSF; Nordic Biosite) at 37°C and 5% $CO_2$. All cell lines tested negative for *Mycoplasma* but were not authenticated in our laboratory. Agonistic rat-anti-mouse CD40 (clone: FGK4.5) and rat IgG2a (clone: 2A3) were purchased from BioXCell and diluted in PBS. Depletion of $CD8^+$ cells was performed by injecting 20 μg/g body weight rat-anti-mouse CD8a (clone: 53.6.72, BioXCell) intraperitoneally on days 0, 1, 2, 6, 10, and 14. $CD8^+$ T-cell depletion was confirmed by flow cytometry by staining with clone 53-5.8 (data not shown).

### Animals

C57BL/6 mice were obtained from Taconic M&B. $CD40^{-/-}$ knockout C57BL/6 mice were obtained from The Jackson Laboratory (B6.129P2-Cd40$^{tm1Kik}$/J). Animals were housed at the Rudbeck Animal Facility and cared for by the staff according to regional regulation. All animal experiments were approved by the Uppsala Animal Ethics Committee (Dnr: C303/9, C21/10, C11/11, and C38/11).

### *In vivo* experimental design

Several variants of subcutaneous MB49 tumor models were used in this study. In the majority of experiments, $2.5 \times 10^5$ cells were injected in the right flank of C57BL/6 mice with therapy conducted on days 7, 10, and 13. For the biodistribution study, $2 \times 10^5$ MB49 cells were inoculated in the right and left flank on day 0. Ten days later, 30 μg of radioactively labeled $^{125}$I-CD40 antibody and $^{131}$I-rat IgG2a were mixed and injected once intravenously or peritumorally at the right side of the tumor. Animals were sacrificed 4, 24, 48, and 72 hours after injection, organs were isolated, and their radioactivity was measured. Radioactivity of $^{125}$I-CD40 antibody was measured in the energy window of 3 to 6 keV and $^{131}$I-rat IgG2a of 100 to 380 keV. In the last tumor model investigating the systemic effects of low-dose anti-CD40 therapy, $2.5 \times 10^5$ MB49 cells were injected in the right flank on day 0 and close to the left shoulder on day 1. Therapy was injected peritumorally at the primary tumor, subcutaneously in the nontumor flank, or intravenously every third day for a total of three times. To keep a similar distance between injection site and the distant tumor as well as to reduce passive diffusion of antibodies in the void space of the skin, animals injected with subcutaneous anti-CD40 antibody in the nontumor flank had both tumors inoculated on the same side of the animal, opposite to the injection side (Fig. 2E). Antibody solution was administered in 100 μL. Tumor growth and survival were monitored throughout the experiment using a caliper and tumor size was calculated by the ellipsoid volume formula: $= 4/3 \times \pi \times a$ (radius of length) $\times$ $b$ (radius of width) $\times$ $c$ (radius of depth). Mice were sacrificed if the tumor exceeded 1 $cm^3$ or if ulcers developed. Tumor rechallenge, by injection of $2.5 \times 10^5$ MB49 (contralateral flank) and LLC-1 cells (right foreleg), was performed on mice that had been tumor free for over 100 days.

### Labeling of antibodies

$^{125}$I and $^{131}$I were purchased from PerkinElmer. Chloramine-T and sodium metabisulfite were from Sigma Chemical Company. Chloramine-T and sodium metabisulfite solutions were prepared immediately before use. The radiochemical purity of the labeled antibody construct was analyzed using instant thin layer chromatography (ITLC) on 150-771 DARK GREEN, Tec-Control Chromatography Strips from Biodex Medical System. Distribution of radioactivity along the ITLC strips was measured using a Cyclone Storage phosphor system and analyzed with the OptiQuant image analysis software (PerkinElmer). Size-exclusion chromatography was performed on disposable NAP-5 columns (Amersham Pharmacia Biotech AB) according to the manufacturer's instructions. The radioactivity was measured using an automated gamma-counter with a 3-inch NaI (Tl) detector (1480 Wizard; Wallac Oy). Monoclonal antibodies were labeled using Chloramine-T as an oxidant according to the following protocol. Anti-CD40 antibody was labeled with $^{125}$I. An antibody solution in PBS (40 μg, 4–2 μL) was mixed with radioiodine stock solution (2–5 μL, 5–10 MBq) and 40 μL PBS. The reaction was initiated by adding Chloramine-T (20 μg, 1 mg/mL in PBS). After 2-minute incubation at ambient temperature, the reaction was terminated by adding sodium

Published OnlineFirst October 21, 2013; DOI: 10.1158/2326-6066.CIR-13-0067



metabisulfite (40 μg, 2 mg/mL in PBS). Rat IgG2a was labeled with $^{131}$I in a similar way. Radiolabeled antibodies were purified from unreacted radioiodine and low-molecular-weight components of the reactive mixture using size-exclusion chromatography on disposable NAP-5 columns. Radiochemical purity of the labeled antibodies was determined by radio-ITLC eluted with acetone:water (8:2) mixture. The yields were in the range of 65% to 75%. After size-exclusion purification, the radiochemical purity of the antibodies was more than 99.5%.

### Trichloroacetic acid precipitation

Trichloroacetic acid (TCA) precipitates high-molecular-weight molecules. Precipitation was carried out according to the protocol described previously (22). Briefly, on top of 300 μL of carrier solution (PBS/0.02% BSA, w/v), 200 μL of plasma was added. Then, 500 μL of ice-cold 20% TCA/$H_2O$ (w/v) solution was added to precipitate high-molecular-weight molecules in the plasma. Tubes were centrifuged and separated before individual measurement for radioactivity using an automated gamma-counter with a 3-inch NaI (Tl) detector.

### Internalization of anti-CD40 antibody

Anti-CD40 antibody was conjugated with Alexa Fluor 488 protein-labeling kit according to the manufacturer's protocol (Invitrogen). The functionality of the labeled antibody was verified by staining of A20 cells (data not shown). D1 cells were seeded in 96-well plates and stimulated overnight with 1 μg/mL lipopolysaccharide (LPS; Sigma) to upregulate the expression of the CD40 receptor. Cells were incubated with 0.1 μg/mL Alexa Fluor 488-conjugated anti-CD40 antibody for 15 or 60 minutes at 37°C or 4°C or left untreated before being fixed in 3%PFA/PBS on ice, and then washed twice in 0.5%PFA/PBS. Trypan blue (Invitrogen) was added just before flow-cytometric analysis to quench any surface-bound antibody. Samples were run in triplicates.

### *In vivo* CD40 expression

To evaluate which cell populations could potentially act as targets for anti-CD40 therapy, naïve animals were injected subcutaneously with 30 μg of anti-CD40 one, two, or three times at 3-day intervals. Four hours postinjection the spleen and (pooled) inguinal lymph nodes were harvested and digested with Liberase TL (Roche) for 15 minutes at 37°C. The Liberase-treated tissue was passed through a MESH membrane, blocked for FcγR (TruStain fcX), and subsequently stained for CD11c (clone: N418), CD11b (clone: M1/70), F4/80 (CI:A3-1), B220 (RA3-6B2), and CD40 (3/23; all antibodies are from BioLegend). Staining with antibody clone 3/23 was not hampered by the presence of the therapeutic clone FGK4.5 on cells (data not shown). The following cell types were investigated: B cells ($B220^+$, $CD11b^-$, $CD11c^-$, and $F4/80^-$), conventional dendritic cells (cDC; $CD11c^{hi}$, $CD11b^{+/-}$, and $B220^-$), medullary macrophage (MΦ; $CD11c^{low/int}$, $CD11b^+$, $B220^-$, and $F4/80^+$), and subcapsular sinus MΦ ($CD11c^{low/int}$, $CD11b^+$, $B220^-$, and $F4/80^-$). Samples were analyzed in a FACSCanto II cytometer (BD Biosciences). Data analysis was performed with FlowJo software (TreeStar).

### Haptoglobin and anti-rat IgG2a antibody measurements

Blood was collected by tail vein incision and serum was stored at −80°C. Mouse haptoglobin was detected by ELISA according to the manufacturer's protocol (Life Diagnostics, Inc.). Quantification of circulating anti-CD40 antibody was performed by ELISA. Briefly, wells were coated with 1.25 μg/mL anti-rat IgG2a (clone: MARG2a-1; Serotec) and blocked with 3% milk powder before the addition of samples (1:10–1:75 dilution). Horseradish peroxidase (HRP)–conjugated mouse-α-rat κ/λ light chain (MARK-1/MARL-15; Serotec) was used for detection. Substrate (Super Signal pico chemoluminescence; Pierce) was added before the luminescence was measured with an ELISA reader (Fluostar optimal; LabVision). Samples were run in duplicates.

### Statistical analysis

Survival data were plotted by the Kaplan–Meier method and analyzed by the log-rank test. When applicable, the D'Agostino and Pearson omnibus normality test was used before selection of statistical test. Where indicated, the difference between groups was evaluated using unpaired $t$ test or paired $t$ test. $P$ values less than 0.05 were considered significant. Asterisks indicate the confidence interval (*, $P < 0.05$; **, $P < 0.01$; ***, $P < 0.001$). Statistical analyses were performed using GraphPad prism software (GraphPad Software, Inc.).

## Results

### Local low-dose anti-CD40 therapy results in improved survival and reduced toxicity compared with systemic treatment

To our knowledge, a direct comparison between local and systemic administration of equal doses of anti-CD40 therapy has not been performed. Ten and 30 μg of peritumorally delivered antibody prolonged survival compared with control animals, whereas systemic therapy of the same doses did not (Fig. 1A, top and middle). Only the highest systemic dose (100 μg) resulted in prolonged survival that was similar to that in the local therapy-treated animals (Fig. 1A, bottom).

Several immune-related side effects have been observed with systemic anti-CD40 antibody therapy in both preclinical models (23) and patients (19). In our current study, levels of circulating therapeutic antibody were measured 4 hours after each injection (Fig. 1B). For all doses and administration routes, the serum maximum level of anti-CD40 antibody occurred after the second injection, with the highest concentrations in animals treated systemically with 30 or 100 μg of antibodies. Local immunotherapy led to reduced serum levels of antibody in all groups compared with that of the equivalent systemic dose. The initial reduction in systemic antibody levels could translate to reduced toxicity. In the current studies, we used haptoglobin, an acute phase protein produced mainly by the liver, as a marker for systemic inflammation (24–26). Serum levels of haptoglobin were measured 24 hours after the first dose, and elevated levels were detected in mice treated with intravenous injections (Fig. 1C). Local injection of the same dose did not elevate haptoglobin levels to the same degree, and

Published OnlineFirst October 21, 2013; DOI: 10.1158/2326-6066.CIR-13-0067



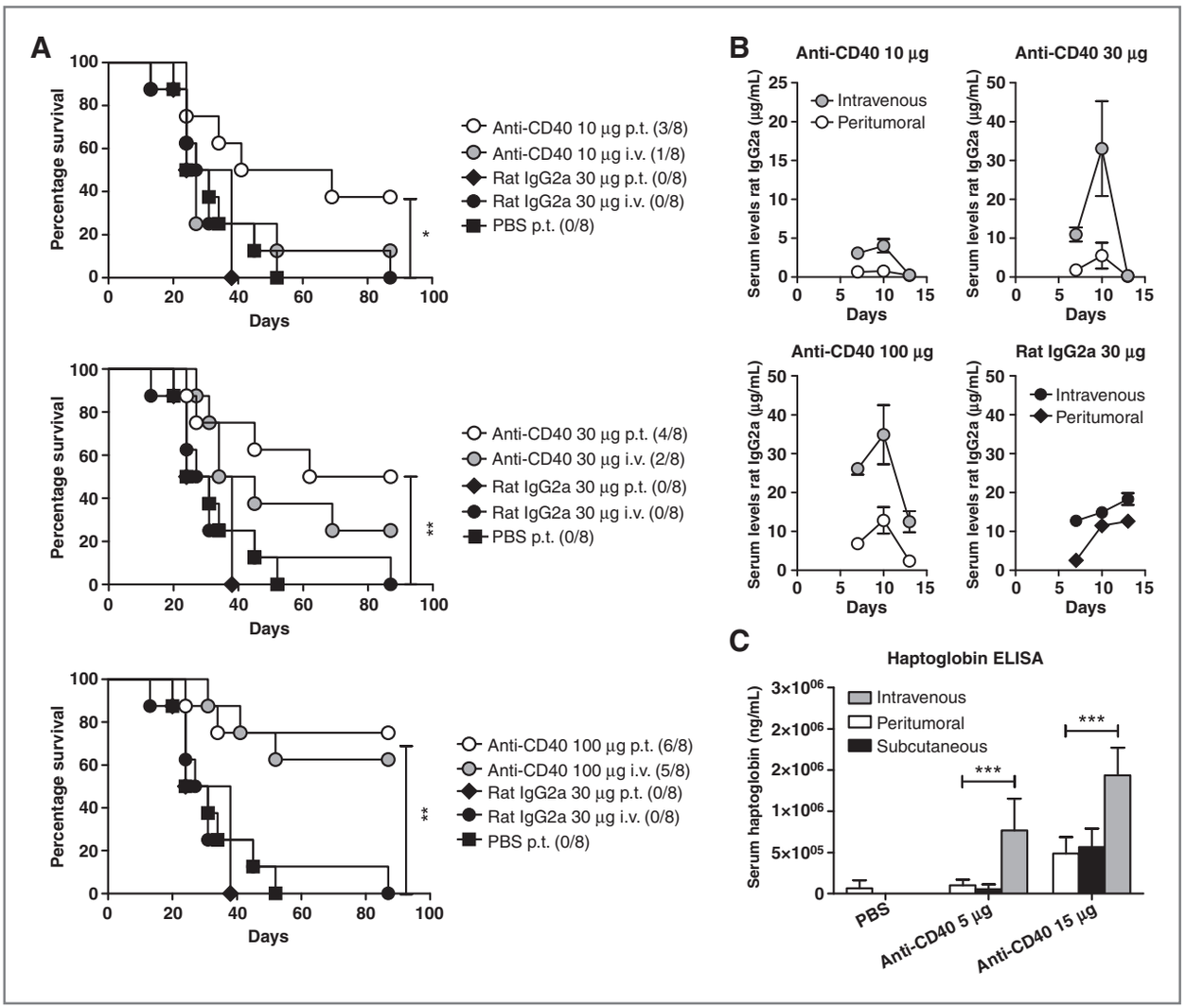


Figure 1. Local low-dose anti-CD40 therapy is superior to systemic treatment and reduces circulating antibodies and haptoglobin levels. A, C57BL/6 mice were treated as described in Materials and Methods. Survival data are shown for 8 mice/group (log-rank test). B, blood was collected for kinetic analysis 4 hours after every treatment occasion from mice in A and analyzed with ELISA. Data are shown as mean ± SEM of 6 mice/group and time point. Samples were run in duplicates. C, serum was isolated 24 hours after the first therapy occasion of mice in Fig. 2F and analyzed for haptoglobin levels with ELISA. Data are shown as mean ± SD of 9 mice/group and time point (Student *t* test; *, $P < 0.05$; **, $P < 0.01$; ***, $P < 0.001$). p.t., peritumorally.

neither peritumorally nor intravenously administered irrelevant antibody affected haptoglobin levels (data not shown).

The local low-dose strategy was also assessed using the fast-growing B16-F10 tumor model where tumor growth inhibition was evident compared with control animals (Supplementary Fig. S1A). Furthermore, weekly dosing with peritumorally low-dose anti-CD40 was evaluated in a high MB49-tumor burden model. Both the weekly and the 3-day interval treatment schedule restrained tumor growth. However, elevated levels of ADA were detected in the serum already after the second injection of anti-CD40 antibody on a weekly schedule, which was not seen using the 3-day interval protocol (data not shown).

### $CD8^+$ T cells, host CD40 expression, and tumor antigen at the injection site are all required for full therapeutic efficacy

CD40 is widely expressed on different cell types *in vivo*, and a variety of cells have been proposed to be effectors in CD40 agonistic therapy. Macrophages (27, 28), B cells (29), natural killer (NK) cells indirectly (30), and T cells (20) via dendritic cell activation have been suggested to play crucial roles in tumor eradication. We asked whether our local low-dose administration of anti-CD40 antibody would depend on the presence of $CD8^+$ T cells by using cell-depletion experiments. $CD8^+$ cells were necessary for optimal antitumor effects as depleted mice showed no survival benefit compared with controls (Fig. 2A). Furthermore, depletion of

Published OnlineFirst October 21, 2013; DOI: 10.1158/2326-6066.CIR-13-0067



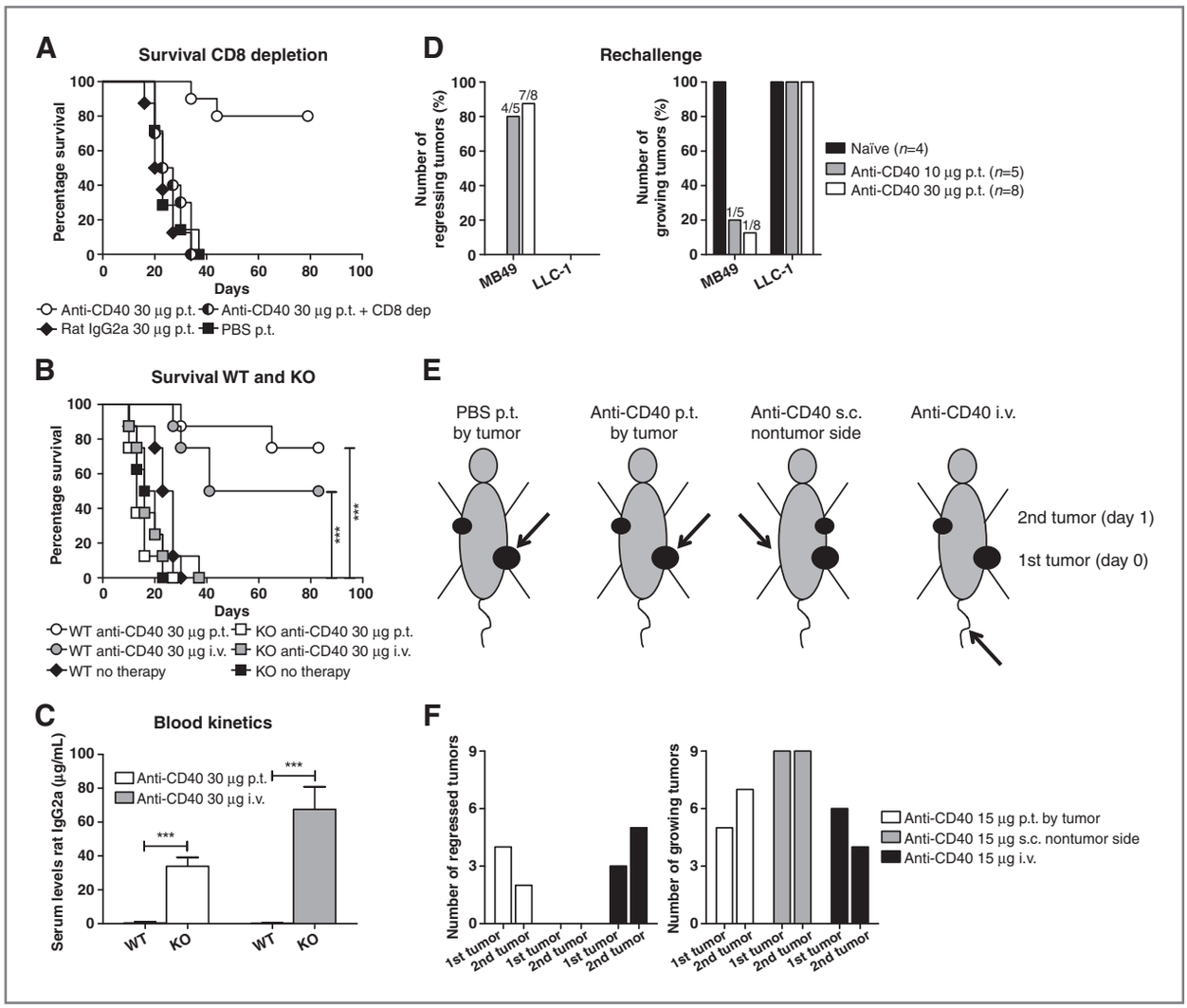


Figure 2. Successful peritumoral (p.t.) anti-CD40 therapy is dependent on $CD8^+$ cells, host CD40 expression, and tumor antigen by the injection site. C57BL/6 mice were treated as described in Materials and Methods. A, one therapy group was depleted of $CD8^+$ cells. Survival data of 7 to 10 mice/group are shown. B, anti-CD40 therapy was evaluated in wild-type (WT) and CD40 knockout (KO) C57BL/6 animals. Survival curve is shown for 8 mice/group (log-rank test). C, blood kinetic analysis of serum anti-CD40 antibody 4 hours after the last treatment was measured with ELISA. Data are shown as mean ± SD of 5 mice/group (Student *t* test). D, complete responders to local anti-CD40 therapy were rechallenged with $2.5 \times 10^5$ MB49 and LLC-1 cells to evaluate tumor-specific memory. Naïve mice, not age-matched, were inoculated with both cell lines on the right and left flank, respectively. Data are visualized as percentage of regressing or progressively growing tumors. E, MB49 cells were injected on day 0 and on day 1 of individual mice and treated with 15 μg of anti-CD40 antibody (black arrow) every third day starting on day 7 according to the illustration. F, tumor growth of animals presented as number of regressed or growing tumors per treatment group ($n = 9$; ***, $P < 0.001$).

$CD4^+$ T cells yielded variable results as 6 of 10 animals experienced rapidly growing tumors and 3 of 10 had recurrence of tumors after initial remission (data not shown). Removal of regulatory T cells (Treg) cannot be excluded. Previous studies have shown that the CD40–CD40L interaction not only activates APCs but generates a direct antitumor effect in CD40-expressing tumors (12, 31). Throughout this study, MB49 cells presented a negligible amount of CD40 expression when staining with the therapeutic antibody clone (data not shown). Despite this result, we wanted to exclude tumor cell death induced directly by the antibody and therefore subjected tumor-bearing C57BL/6 wild-type (WT) and $CD40^{-/-}$ knockout mice to local or systemic treatment. Figure 2B shows that host CD40 expression is required for effective anti-CD40 therapy regardless of administration route. The knockout mice had elevated levels of circulating anti-CD40 antibody 4 hours after the last treatment compared with WT animals (Figs. 2C and 1B).

To establish tumor-specific memory after local anti-CD40 therapy, animals exhibiting complete tumor regression were rechallenged with MB49 cells and LLC-1 (Fig. 2D). LLC-1 tumors grew progressively in both naïve and cured mice,

Published OnlineFirst October 21, 2013; DOI: 10.1158/2326-6066.CIR-13-0067



whereas progressive growth of MB49 tumors was only seen in naïve animals.

Because low but detectable levels of anti-CD40 antibody were found in the blood after local administration, we wanted to investigate whether distant tumors could be cleared and whether tumor antigens are required at the injection site, as demonstrated earlier by Fransen and colleagues (20). To minimize systemic antibody dissemination, 15 μg of anti-CD40 antibody was used but without a slow-release formulation. A twin-tumor model was set up by engrafting MB49 cells in the right flank on day 0 and close to the left shoulder on day 1 (Fig. 2E). As visualized in Fig. 2F, anti-CD40 antibody needs to be injected in close proximity to a tumor (or systemically) to affect both the treated site as well as the distant tumor. Therapy injected solely in the skin (nontumor side) did not inhibit tumor growth. For individual tumor growth, see Supplementary Fig. S1B.

We determined the level of effector cytokines in the serum and registered a dose-dependent elevation of serum IFN-γ, IP-10, and TNF-α 4 hours after the second dose using all administration routes (data not shown). In agreement with the clinical observation using the humanized CP-870,893 antibody (16, 19), we registered a transient B-cell depletion after a single injection of anti-CD40 antibody (data not shown), which was less pronounced after local administration.

### Local and systemic anti-CD40 antibody accumulates in secondary lymphoid organs

To investigate the *in vivo* biodistribution of anti-CD40 agonist or control antibody upon local versus systemic administration, we measured antibody accumulation in target organs after a single injection. For this purpose, anti-CD40 antibody was labeled with $^{125}$I and the irrelevant isotype with $^{131}$I to allow simultaneous measurement in the same animal by gamma-spectrometry. The binding-specificity of the $^{125}$I-CD40-specific antibody was confirmed before experimental initiation (Supplementary Fig. S2A). An equal dosage mixture of $^{125}$I-CD40–specific and $^{131}$I-rat IgG2a control antibodies was injected into mice carrying a tumor in each flank either peritumorally at the right side tumor or intravenously. At 4, 24, 48, and 72 hours after injection, animals were sacrificed, organs isolated, and radioactivity measured. A high accumulation of $^{125}$I-CD40–specific antibody was detected in the spleen 4 hours after injection followed by a decrease over time (Fig. 3A). $^{131}$I-rat IgG2a control antibody uptake in the spleen was significantly lower.

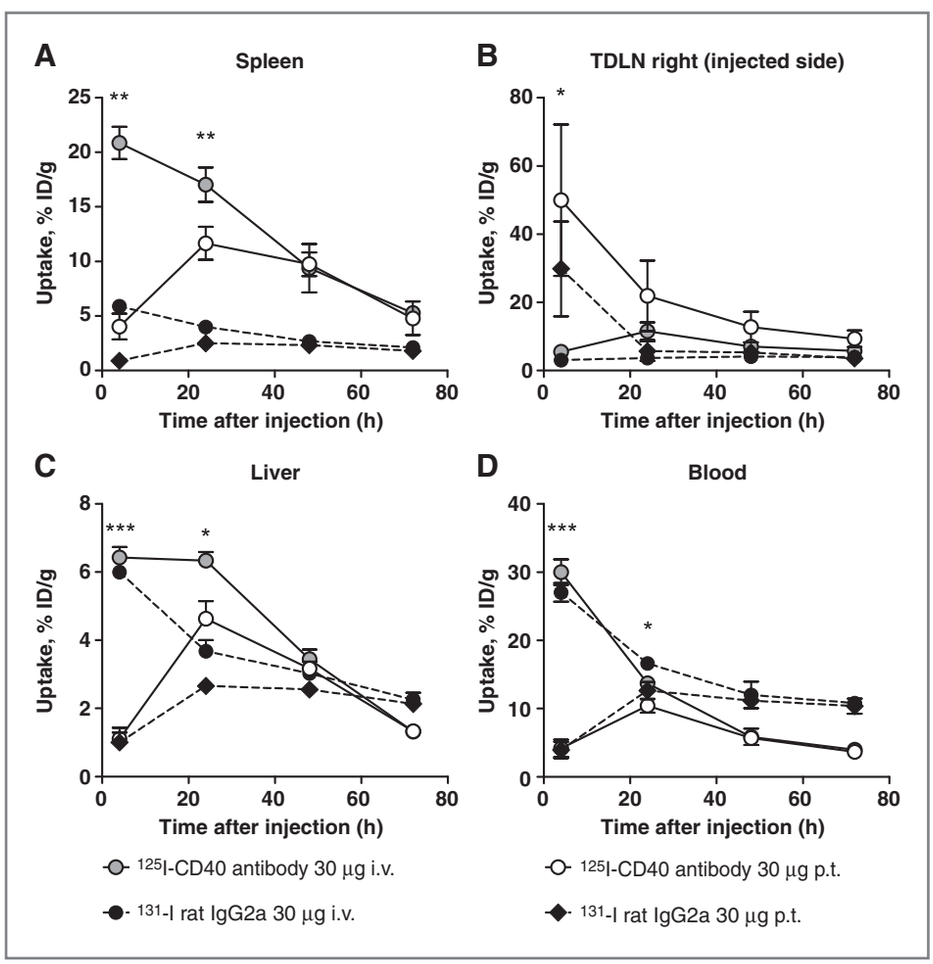


Figure 3. CD40 agonist accumulates in secondary lymphoid organs. C57BL/6 mice were treated as described in Materials and Methods. Target organs (A–D) were isolated 4, 24, 48, and 72 hours posttreatment, measured for accumulated radioactivity, and visualized as percentage injected dose/g tissue (%ID/g). Statistical significance is calculated between intravenous and peritumoral (p.t.) administrations (mean ± SD of 4 mice/group; Student paired *t* test. *, $P < 0.05$; **, $P < 0.01$; ***, $P < 0.001$).

Published OnlineFirst October 21, 2013; DOI: 10.1158/2326-6066.CIR-13-0067



The highest amount of locally administered anti-CD40 antibody was found in the spleen at 24 hours, followed by a decline. The uptake of $^{131}$I-rat IgG2a control antibody in the same animal was significantly lower than that of the $^{125}$I-CD40–specific antibody (Fig. 3A). The spleen accumulation was significantly lower after peritumoral administration than after intravenous injection at 4 and 24 hours. At subsequent time points, the radioactivity uptakes were equal for both administration routes. Anti-CD40 antibody uptake in the right tumor-draining lymph node (TDLN) after peritumoral injection was much higher at 4 hours as compared with that of systemic administration (Fig. 3B). Systemic delivery of anti-CD40 antibody induced a more pronounced accumulation in the liver compared with peritumoral injection at 4 and 24 hours (Fig. 3C). Furthermore, local administration resulted in a lower initial antibody concentration in the blood at 4 and 24 hours (Fig. 3D), in agreement with our ELISA results. We found that the concentration of radioactivity in the plasma was higher than in whole blood, indicating minor (if any) binding of $^{125}$I-CD40 to blood cells (Supplementary Fig. S2B). In summary, peritumoral delivery significantly reduced anti-CD40 antibody concentrations in the spleen, liver, and blood compared with intravenous injection at both 4 and 24 hours after injection.

Figure 4 shows antibody uptake for selected target organs at 4 (Fig. 4A) and 24 hours (Fig. 4B). Results from the 48- and 72-hour time points are visualized in Supplementary Fig. S3. Statistical differences between the anti-CD40 and the control antibody and between the two administration routes in all organs investigated are summarized in Supplementary Tables S1–S4.

**Repeated anti-CD40 therapy modulates CD40 expression as well as immune cell distribution in lymphoid tissue**

The anti-CD40–specific antibody showed a more rapid clearance from the blood than the control antibody. To verify how much of the blood-borne radioactivity was still conjugated, we performed a TCA precipitation assay. Although almost all $^{131}$I was conjugated to rat IgG2a in both treatment groups during the entire study period, a decrease of activity in the high-molecular-weight form was detected for the $^{125}$I-CD40–specific antibody conjugate (Fig. 5A). This suggests that the anti-CD40 antibody was efficiently sequestered from the circulation due to specific interaction followed by subsequent internalization and catabolism. This could be by active uptake in cells and we therefore incubated fluorophore-conjugated anti-CD40 antibody with CD40-expressing dendritic cells for 15 or 60 minutes and subsequently quenched surface-bound antibodies. Our findings imply that anti-CD40 antibody is internalized within 15 minutes (Fig. 5B). As several cell populations in lymphoid organs, including B cells, CD8$^+$, CD8$^-$ cDCs, macrophages, NK cells, NKT cells, and activated CD4$^+$ T cells, can act as potential targets for CD40-activating therapy, we investigated the expression of CD40 on immune cells from the inguinal lymph nodes

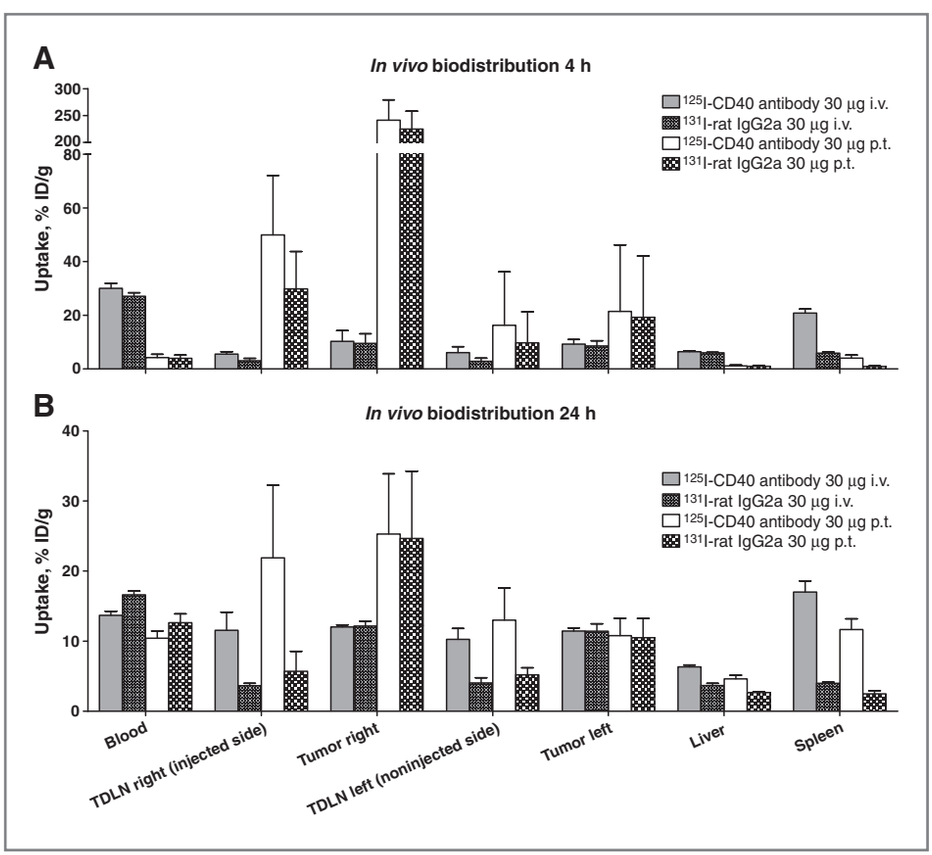


Figure 4. *In vivo* biodistribution of target organs 4 and 24 hours after injection of $^{125}$I-CD40–specific and $^{131}$I-rat IgG2a control antibody. Radioactive uptake of target organs (A) 4 and (B) 24 hours after injection of animals in Fig. 3. Data are presented as percentage injected dose/g tissue (%ID/g, mean ± SD of 4 mice/group). Statistical differences between anti-CD40 and rat IgG2a and between the two administration routes are depicted in Supplementary Table S1 (4 hours) and S2 (24 hours). p.t., peritumorally.

Published OnlineFirst October 21, 2013; DOI: 10.1158/2326-6066.CIR-13-0067



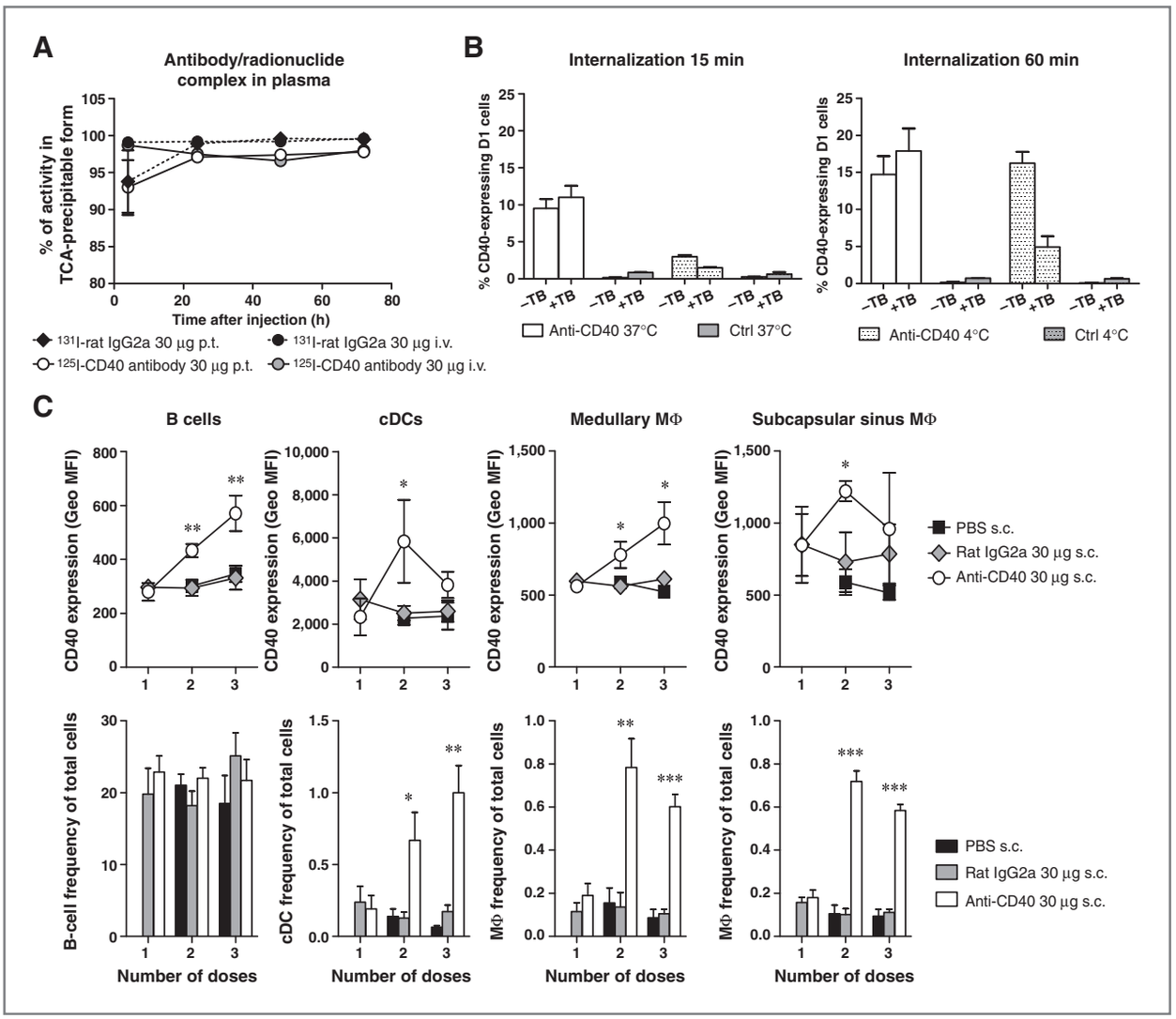


Figure 5. CD40-specific antibody is catabolized and rapidly internalized by CD40-expressing cells. A, plasma collected during the biodistribution study was subjected to TCA precipitation (mean ± SD of 4 mice/group). B, LPS-stimulated D1 cells were incubated with Alexa Fluor 488–conjugated anti-CD40 antibody for 15 or 60 minutes at 37°C or 4°C or left untreated. Just before flow-cytometric analysis, Trypan blue (+TB) was added to quench any surface-bound antibody. Samples were run in triplicates (mean ± SD). C, CD40-expressing target cell populations were investigated in inguinal lymph nodes after one, two, or three doses of anti-CD40 antibodies (3-day interval scheme), CD40 expression, and cell distribution were analyzed 4 hours after injection. Top, CD40 expression based on geometric mean fluorescence intensity (Geo MFI); bottom, the frequency of total cells. Statistical significance is calculated between rat IgG2a and anti-CD40 (mean ± SD of 3 mice/group; Student *t* test; *, $P < 0.05$; **, $P < 0.01$; ***, $P < 0.001$). p.t., peritumorally.

(Fig. 5C) and the spleen (Supplementary Fig. S2C) 4 hours after one, two, or three subcutaneous injections of 30 μg anti-CD40. Lymph node B cells, cDCs, and macrophages all increased their surface expression of CD40 in a dose-dependent manner following anti-CD40 injections (Fig. 5C, top). Also, elevated numbers of total cDCs and macrophages were found in response to therapy (Fig. 5C, bottom). For the spleen, the results were slightly more variable; however, there was an apparent drop in the numbers of monocyte-derived macrophage and dendritic cells after the third injection (Supplementary Fig. S2C).

## Discussion

Effective tumor immunotherapy needs to overcome the challenge of poorly immunogenic antigens (32), lack of danger signals (33), and the presence of an immunosuppressive milieu caused by both the tumor and the infiltrating cells (34). CTLs exhibit poor activation by improperly activated or immature dendritic cells (35, 36). The general principle of anti-CD40 antibody in tumor immunotherapy, as demonstrated earlier, is to create a Th-independent activation of CTLs by direct licensing of dendritic cells (10, 11, 37).

Published OnlineFirst October 21, 2013; DOI: 10.1158/2326-6066.CIR-13-0067



We used peritumoral injection as the local administration route in this study because this route confers minimal mechanical stimulation of the tumor. A comparison with intratumoral injection in tumors using the same treatment protocol as in Fig. 1 showed that there was no advantage to this approach over peritumoral delivery (data not shown).

A survival benefit was observed for mice treated with local low-dose anti-CD40 antibody (10 and 30 μg) compared with the same dose delivered systemically, which indicates that systemic injections in this dose range result in a low concentration of antibody in the tumor/TDLN axis that is insufficient for CTL activation. As no difference in survival was noticed at the 100 μg dose between the two administration routes, a high level of circulating antibody could potentially overcome this problem but with increased side effects. We registered elevated levels of serum haptoglobin as a sign of systemic inflammation (24–26) already at low intravenous anti-CD40 antibody doses. Furthermore, liver exposure to the antibody was appreciably higher after intravenous injection compared with peritumoral injection. These data suggest that local low-dose antibody delivery can reduce liver toxicity compared with systemic therapy, which could be valuable in the clinic as patients often display metastatic disease that could be targeted by recruiting immune cells rather than the anti-CD40 antibody itself.

Our finding that $CD8^+$ T cells are important for the antitumor effects of anti-CD40 therapy is consistent with data from other groups (23). However, CD40 activation can target many other cell types, such as macrophages, which could participate in tumor eradication. The differences observed may be dose- or animal model-related. CD40-stimulating therapy can have a direct antitumor effect on CD40-expressing tumors by inducing apoptosis (12, 31). Throughout this study, MB49 cells presented a negligible level of CD40 expression based on staining with the therapeutic antibody. Notably, when staining with the anti-CD40 antibody clone 3/23 on MB49 cells, CD40 expression could be visualized. To confirm that locally delivered therapy was fully dependent on host CD40 expression, we made use of $CD40^{-/-}$ knockout animals. Endogenous CD40 expression was required for full therapeutic effect regardless of injection site. We also confirmed the antitumor effects in the CD40-negative B16 melanoma model in WT mice. In contrast with our MB49 model, human bladder cancer cells usually present CD40 expression compared with the CD40-negative urothelium (38). Also, CD40 ligation in the form of cell-surface bound CD40L or Fcγ receptor cross-linked anti-CD40 antibody induces apoptosis in transitional bladder carcinoma (39). Engaging both the direct- and indirect-killing mechanisms for the treatment of bladder cancer could be even more efficient. These observations, together with the convenient intravesical access of bladder cancer, make this tumor a suitable target for localized anti-CD40 therapy.

The presence of tumor antigen in close proximity to the anti-CD40 antibody injection for systemic tumor eradication was demonstrated by Fransen and colleagues (20). Our data strengthen these results and extended them further by showing substantiated levels of the antibody in the regional lymph nodes, both at the injection site and at the nontreated side. These results suggest that tumor-localized anti-CD40 therapy can be effective for targeting disseminated bladder cancer.

We performed *in vivo* biodistribution studies and detected high initial levels of anti-CD40 antibody in the spleen after intravenous injection and in the right TDLN after peritumoral delivery. However, at later time points, accumulation of anti-CD40–specific antibody was observed in these lymphoid organs with both administration routes, which may reflect the abundance of CD40-positive target cells. The drainage of both anti-CD40 antibody and tumor antigens to the same TDLN could increase the possibility of tumor-specific T-cell triggering by locally activated APCs as indicated by Fransen and colleagues (20). Therefore, our demonstration of a high concentration of anti-CD40 antibody in the TDLN seems crucial for optimal anti-CD40 antibody therapy. In addition, our *in vivo* study revealed increased CD40 expression and expansion of target APCs in the lymph node after repeated anti-CD40 injections, likely reflecting that the lymph node is a key player in local anti-CD40 therapy.

The kinetics of peritumorally and intravenously delivered anti-CD40 antibody in the blood was determined by ELISA and by radiolabeled antibody. Locally injected antibody reached its maximum after 24 hours followed by exponential decrease. A subsequent injection caused even higher serum levels for both administration routes, but after the third treatment (day 13), anti-CD40 antibody levels were low or nondetectable. Drug elimination could be due to the induction of ADA, the inability of ELISA to measure ADA complexes, and/or increased cell/tissue expression of CD40 leading to rapid antibody clearance. ADA-dependent serum clearance has also been suggested in preclinical studies using cynomolgus monkeys (40). Furthermore, elimination of $^{125}$I-CD40–specific antibody from the circulation was faster than that for the control, which likely reflects specific binding outside the blood (and not ADA-associated elimination) as these animals received only a single injection. We found higher amounts of circulating anti-CD40 antibody in CD40 knockout mice compared with WT indicative of target-specific sequestering of the antibody. These findings correlate well with the clinical findings of CD40-agonistic antibodies, such as the CP-870,893 antibody (19), and the weak CD40 agonist SGN-40 antibody (41), both display relatively short half-life. This suggests that there may be a target-specific clearance from the blood in humans, and it has been speculated that this reflects a large sink of CD40 molecules *in vivo* (16). Our results demonstrate that, in mice, this sink is primarily located in the secondary lymphoid organs. In the lymph node and spleen, the CD40-expressing cells are B cells, $CD8^+$, $CD8^-$ cDCs, a variety of macrophages, NK cells, NKT cells, and activated $CD4^+$ T cells. Interestingly, we found that macrophages as well as dendritic cells both increased in numbers and upregulated their CD40 expression subsequent to repeated CD40 agonist injections, whereas B cells only upregulated CD40 expression in the lymph node. The result was slightly more variable for spleen cells, but the drop in monocyte-derived macrophages as well as dendritic cells could reflect a recruitment of APCs into the lymph node and/or tissues. Furthermore, our data showed that anti-CD40 antibody was rapidly (15 minutes) internalized by CD40-expressing dendritic

Published OnlineFirst October 21, 2013; DOI: 10.1158/2326-6066.CIR-13-0067



cells, most likely contributing to reduced serum levels of the antibody. In our hands, tumor-targeting seems minimal as no major specific accumulation of radiolabeled anti-CD40 could be detected. This is also in agreement with the lack of CD40-staining on MB49 cells by flow-cytometric analyses using the labeled therapeutic antibody. The correlation between blood and tumor, where late time points (48 and 72 hours) demonstrate specific accumulation of irrelevant antibody, further supports the target-specific sequestering of antibodies.

Systemic anti-CD40 therapy has been used extensively in the clinic (16, 17, 19, 41) and in preclinical models, with immune-related adverse events such as systemic cytokine release syndrome and liver toxicity. Lately, the focus has shifted toward local administration, through which doses and consequently toxicity can be reduced, but potentially retaining the efficacy of the systemic antitumor effects (20, 23, 29, 42–44).

In summary, this is to our knowledge the first study exploring local and systemic anti-CD40 therapy side by side in a dose-comparison study and including an in-depth analysis of antibody biodistribution *in vivo*. Our data support the use of local low-dose delivery of anti-CD40 antibody as an alternative to systemic high-dose therapy. This should be a relevant immunotherapeutic approach in combinatorial treatments with current immunomodulatory agents for localized and disseminated bladder cancer, and possibly other tumor types as well.

## Disclosure of Potential Conflicts of Interest

L.C. Sandin, P. Ellmark, and S.M. Mangsbo have ownership interest in a patent. T.H. Tötterman has an ownership interest in a patent and is a consultant/advisory board member for Alligator Bioscience, Inc. and Immuvent Inc. No potential conflicts of interest were disclosed by the other authors.

## Authors' Contributions

**Conception and design:** L.C. Sandin, P. Ellmark, V. Tolmachev, T.H. Tötterman, S.M. Mangsbo

**Development of methodology:** L.C. Sandin, V. Tolmachev, T.H. Tötterman, S.M. Mangsbo

**Acquisition of data (provided animals, acquired and managed patients, provided facilities, etc.):** L.C. Sandin, A. Orlova, E. Gustafsson, V. Tolmachev, T.H. Tötterman, S.M. Mangsbo

**Analysis and interpretation of data (e.g., statistical analysis, biostatistics, computational analysis):** L.C. Sandin, A. Orlova, E. Gustafsson, V. Tolmachev, T.H. Tötterman, S.M. Mangsbo

**Writing, review, and/or revision of the manuscript:** L.C. Sandin, P. Ellmark, V. Tolmachev, T.H. Tötterman, S.M. Mangsbo

**Administrative, technical, or material support (i.e., reporting or organizing data, constructing databases):** L.C. Sandin, A. Orlova, E. Gustafsson, V. Tolmachev, T.H. Tötterman, S.M. Mangsbo

**Study supervision:** V. Tolmachev, T.H. Tötterman, S.M. Mangsbo

## Acknowledgments

The authors thank Ann-Charlotte Hellström (IGP) and Anna Rosén (Alligator Bioscience, Inc.) for excellent technical assistance.

## Grant Support

This study was supported by The Swedish Cancer Society (to T.H. Tötterman), the Swedish Research Council (to T.H. Tötterman), and FP7 MCA-ITN 317445 (to S.M. Mangsbo). P. Ellmark was sponsored by the Swedish Research Council (VR-IFA hosted by Lund University).

The costs of publication of this article were defrayed in part by the payment of page charges. This article must therefore be hereby marked *advertisement* in accordance with 18 U.S.C. Section 1734 solely to indicate this fact.

Received May 31, 2013; revised October 16, 2013; accepted October 16, 2013; published OnlineFirst October 21, 2013.

## References

1. Jemal A, Bray F, Center MM, Ferlay J, Ward E, Forman D. Global cancer statistics. CA Cancer J Clin 2011;61:69–90.
2. Kaufman DS. Challenges in the treatment of bladder cancer. Ann Oncol 2006;17(Suppl 5):v106–12.
3. Brincks EL, Risk MC, Griffith TS. PMN and anti-tumor immunity—the case of bladder cancer immunotherapy. Semin Cancer Biol 2013;23:183–9.
4. Kawai K, Miyazaki J, Joraku A, Nishiyama H, Akaza H. Bacillus Calmette-Guerin (BCG) immunotherapy for bladder cancer: current understanding and perspectives on engineered BCG vaccine. Cancer Sci 2013;104:22–7.
5. Lindqvist C, Sandin LC, Fransson M, Loskog A. Local AdCD40L gene therapy is effective for disseminated murine experimental cancer by breaking T-cell tolerance and inducing tumor cell growth inhibition. J Immunother 2009;32:785–92.
6. Mangsbo SM, Sandin LC, Anger K, Korman AJ, Loskog A, Totterman TH. Enhanced tumor eradication by combining CTLA-4 or PD-1 blockade with CpG therapy. J Immunother 2010;33:225–35.
7. Malmstrom PU, Loskog AS, Lindqvist CA, Mangsbo SM, Fransson M, Wanders A, et al. AdCD40L immunogene therapy for bladder carcinoma—the first phase I/IIa trial. Clin Cancer Res 2010;16:3279–87.
8. von Euler H, Sadeghi A, Carlsson B, Rivera P, Loskog A, Segall T, et al. Efficient adenovector CD40 ligand immunotherapy of canine malignant melanoma. J Immunother 2008;31:377–84.
9. van Kooten C, Banchereau J. CD40-CD40 ligand. J Leukoc Biol 2000;67:2–17.
10. Bennett SR, Carbone FR, Karamalis F, Flavell RA, Miller JF, Heath WR. Help for cytotoxic-T-cell responses is mediated by CD40 signalling. Nature 1998;393:478–80.
11. Schoenberger SP, Toes RE, van der Voort EI, Offringa R, Melief CJ. T-cell help for cytotoxic T lymphocytes is mediated by CD40–CD40L interactions. Nature 1998;393:480–3.
12. Hess S, Engelmann H. A novel function of CD40: induction of cell death in transformed cells. J Exp Med 1996;183:159–67.
13. Clynes RA, Towers TL, Presta LG, Ravetch JV. Inhibitory Fc receptors modulate *in vivo* cytotoxicity against tumor targets. Nat Med 2000;6:443–6.
14. Oflazoglu E, Stone IJ, Brown L, Gordon KA, van Rooijen N, Jonas M, et al. Macrophages and Fc-receptor interactions contribute to the antitumour activities of the anti-CD40 antibody SGN-40. Br J Cancer 2009;100:113–7.
15. Di Gaetano N, Cittera E, Nota R, Vecchi A, Grieco V, Scanziani E, et al. Complement activation determines the therapeutic activity of rituximab *in vivo*. J Immunol 2003;171:1581–7.
16. Ruter J, Antonia SJ, Burris HA, Huhn RD, Vonderheide RH. Immune modulation with weekly dosing of an agonist CD40 antibody in a phase I study of patients with advanced solid tumors. Cancer Biol Ther 2010;10:983–93.
17. Advani R, Forero-Torres A, Furman RR, Rosenblatt JD, Younes A, Ren H, et al. Phase I study of the humanized anti-CD40 monoclonal antibody dacetuzumab in refractory or recurrent nonHodgkin's lymphoma. J Clin Oncol 2009;27:4371–7.
18. Bensinger W, Maziarz RT, Jagannath S, Spencer A, Durrant S, Becker PS, et al. A phase 1 study of lucatumumab, a fully human anti-CD40 antagonist monoclonal antibody administered intravenously to patients with relapsed or refractory multiple myeloma. Br J Haematol 2012;159:58–66.
19. Vonderheide RH, Flaherty KT, Khalil M, Stumacher MS, Bajor DL, Hutnick NA, et al. Clinical activity and immune modulation in cancer patients treated with CP-870,893, a novel CD40

Published OnlineFirst October 21, 2013; DOI: 10.1158/2326-6066.CIR-13-0067



agonist monoclonal antibody. J Clin Oncol 2007;25:876–83.
20. Fransen MF, Sluijter M, Morreau H, Arens R, Melief CJ. Local activation of CD8 T cells and systemic tumor eradication without toxicity via slow release and local delivery of agonistic CD40 antibody. Clin Cancer Res 2011;17:2270–80.
21. Winzler C, Rovere P, Rescigno M, Granucci F, Penna G, Adorini L, et al. Maturation stages of mouse dendritic cells in growth factor-dependent long-term cultures. J Exp Med 1997;185:317–28.
22. Sundin J, Tolmachev V, Koziorowski J, Carlsson J, Lundqvist H, Welt S, et al. High yield direct 76Br-bromination of monoclonal antibodies using chloramine-T. Nucl Med Biol 1999;26:923–9.
23. van Mierlo GJ, den Boer AT, Medema JP, van der Voort EI, Fransen MF, Offringa R, et al. CD40 stimulation leads to effective therapy of CD40 (−) tumors through induction of strong systemic cytotoxic T lymphocyte immunity. Proc Natl Acad Sci U S A 2002;99:5561–6.
24. Melgar S, Karlsson A, Michaelsson E. Acute colitis induced by dextran sulfate sodium progresses to chronicity in C57BL/6 but not in BALB/c mice: correlation between symptoms and inflammation. Am J Physiol Gastrointest Liver Physiol 2005;288:G1328–38.
25. Duan X, Yarmush DM, Berthiaume F, Jayaraman A, Yarmush ML. A mouse serum two-dimensional gel map: application to profiling burn injury and infection. Electrophoresis 2004;25:3055–65.
26. Wait R, Chiesa G, Parolini C, Miller I, Begum S, Brambilla D, et al. Reference maps of mouse serum acute-phase proteins: changes with LPS-induced inflammation and apolipoprotein A-I and A-II transgenes. Proteomics 2005;5:4245–53.
27. Van De Voort TJ, Felder MA, Yang RK, Sondel PM, Rakhmilevich AL. Intratumoral delivery of low doses of anti-CD40 mAb combined with monophosphoryl lipid a induces local and systemic antitumor effects in immunocompetent and T cell–deficient mice. J Immunother 2013;36:29–40.
28. Beatty GL, Chiorean EG, Fishman MP, Saboury B, Teitelbaum UR, Sun W, et al. CD40 agonists alter tumor stroma and show efficacy against pancreatic carcinoma in mice and humans. Science 2011;331:1612–6.
29. Jackaman C, Cornwall S, Graham PT, Nelson DJ. CD40-activated B cells contribute to mesothelioma tumor regression. Immunol Cell Biol 2011;89:255–67.
30. Turner JG, Rakhmilevich AL, Burdelya L, Neal Z, Imboden M, Sondel PM, et al. Anti-CD40 antibody induces antitumor and antimetastatic effects: the role of NK cells. J Immunol 2001;166:89–94.
31. Eliopoulos AG, Davies C, Knox PG, Gallagher NJ, Afford SC, Adams DH, et al. CD40 induces apoptosis in carcinoma cells through activation of cytotoxic ligands of the tumor necrosis factor superfamily. Mol Cell Biol 2000;20:5503–15.
32. Speiser DE, Miranda R, Zakarian A, Bachmann MF, McKall-Faienza K, Odermatt B, et al. Self antigens expressed by solid tumors do not efficiently stimulate naive or activated T cells: implications for immunotherapy. J Exp Med 1997;186:645–53.
33. Fuchs EJ, Matzinger P. Is cancer dangerous to the immune system? Semin Immunol 1996;8:271–80.
34. Kareva I, Hahnfeldt P. The emerging "Hallmarks" of metabolic reprogramming and immune evasion: distinct or linked?Cancer Res 2013;73:2737–42.
35. Kurts C, Robinson BW, Knolle PA. Cross-priming in health and disease. Nat Rev Immunol 2010;10:403–14.
36. McDonnell AM, Robinson BW, Currie AJ. Tumor antigen cross-presentation and the dendritic cell: where it all begins? Clin Dev Immunol 2010;2010:539519.
37. Ridge JP, Di Rosa F, Matzinger P. A conditioned dendritic cell can be a temporal bridge between a $CD4^+$ T-helper and a T-killer cell. Nature 1998;393:474–8.
38. Cooke PW, James ND, Ganesan R, Wallace M, Burton A, Young LS. CD40 expression in bladder cancer. J Pathol 1999;188:38–43.
39. Bugajska U, Georgopoulos NT, Southgate J, Johnson PW, Graber P, Gordon J, et al. The effects of malignant transformation on susceptibility of human urothelial cells to CD40-mediated apoptosis. J Natl Cancer Inst 2002;94:1381–95.
40. Kelley SK, Gelzleichter T, Xie D, Lee WP, Darbonne WC, Qureshi F, et al. Preclinical pharmacokinetics, pharmacodynamics, and activity of a humanized anti-CD40 antibody (SGN-40) in rodents and non-human primates. Br J Pharmacol 2006;148:1116–23.
41. Hussein M, Berenson JR, Niesvizky R, Munshi N, Matous J, Sobecks R, et al. A phase I multidose study of dacetuzumab (SGN-40; humanized anti-CD40 monoclonal antibody) in patients with multiple myeloma. Haematologica 2010;95:845–8.
42. Todryk SM, Tutt AL, Green MH, Smallwood JA, Halanek N, Dalgleish AG, et al. CD40 ligation for immunotherapy of solid tumours. J Immunol Methods 2001;248:139–47.
43. Khong A, Brown MD, Vivian JB, Robinson BW, Currie AJ. Agonistic anti-CD40 antibody therapy is effective against postoperative cancer recurrence and metastasis in a murine tumor model. J Immunother 2013;36:365–72.
44. Fransen MF, van der Sluis TC, Ossendorp F, Arens R, Melief CJ. Controlled local delivery of CTLA-4 blocking antibody induces $CD8^+$ T-cell–dependent tumor eradication and decreases risk of toxic side effects. Clin Cancer Res 2013;19:5381–9.